

Neurogenin 3	23	3015	-
Bax	21	2989.14	-
Stat3 (pY705), Phospho-Specific	92	2981.25	-
EGF Receptor (activated form)	180	2957.1	-
Dyrk	100	2946.13	-
Caveolin 1	22	2936.99	-
Phospholipase C $\gamma$ (pY783), Phospho-Specific	148	2910.53	-
Reps1	73	2893	-
GAGE	24	2886.06	-
hRAD9	60	2883	-
Chromogranin B	105	2880.22	-
PI3-Kinase p110 $\delta$	110	2874.89	-
Attractin	175	2860.92	-
Stat3-interacting protein 1	92	2844.97	-
Hic-5	50	2841.42	-
Antigen Name	Mol Wt	Signal Intensity (Brain)	Reactivity (Brain)
TEF-1	53	2820.87	-
Stat5	92	2805.1	-
RIP	74	2783.42	-
Sos1	170	2781.88	-
SIP1	32	2780	-
ERp61	58	2764.38	-
GluR d2	111	2748	-
Ref-1	36	2746.9	-
Lamin A/C	65/74	2739.94	-
Paxillin	68	2735.92	-
NSP1	72	2691	-
WRN	162	2671.32	-
CD45	180-220	2657.78	-
Syntaxin 8	27	2652.34	-
PRK1	120	2618.53	-
MAPKAPK-5	54	2616	-
Telethonin	19	2593.22	-
DGKq	110	2576	-
FKBP12	14	2566	-
Caveolin (pY14), Phospho-Specific	22	2553.28	-
4.1N	135/100	2541.35	-
CD3 zeta	180/32	2524.45	-
Sp17	22-23	2520.84	-
b-NAP	145	2519	-
Ninjurin	22	2517.61	-
PKC $\delta$	78	2510	-

p120 Catenin (pY280), Phospho-Specific	120	2504.11	-
Selenocysteine Lyase	47	2502	-
Jagged1	130	2463	-
Kidins220	220	2459	-
TRF2	66	2459	-
JNK (pT183/pY185) Phospho-Specific	43/56	2450.8	-
Calreticulin	60	2446.23	-
BRUCE	528	2439.66	-
Bcl-x	26	2431.31	-
Tapasin	48	2429	-
Stat1 (pY701), Phospho-Specific	84/91	2427.64	-
Antigen Name	Mol Wt	Signal Intensity (Brain)	Reactivity (Brain)
EMeg32	21	2409.79	-
TAO1	116	2397.6	-
LAP2	53	2392.33	-
Casein Kinase II $\alpha/\alpha'$	45	2390.23	-
BRCA1	220	2389.25	-
4.1N	135/100	2361.19	-
Aralar	70	2355.22	-
Syncollin	16	2343.33	-
Adaptin $\alpha$	112	2340	-
Dystrobrevin	87	2337.37	-
UBA2	95	2337	-
Heme Oxygenase 1	32	2328.37	-
Collagen VII $\alpha 1$	290	2301	-
Cadherin-5	130	2296	-
$\beta$ -Dystroglycan (pY892), Phospho-Specific	50	2282.53	-
RACK1	36	2278.25	-
Cox-2	70	2268.83	-
p32	32	2266.77	-
Tyrosine Hydroxylase	58	2239	-
Annexin II	36	2216	-
ZFP-37	67	2213	-
PKC $\gamma$	80	2202.13	-
AKAP-KL	105-130	2196.66	-
Acrp30/Adiponectin	30	2179	-
NMT-2	65	2168	-
Rab5	25	2142	-
MAP4	200-220	2139.83	-
Vesl-1L	45	2124.91	-
Thrombin	77	2122.39	-
Caveolin 1	22	2112.51	-

cGB-PDE/PDE5	95	2106	-
ZO-2	160	2097.11	-
MEKK3	71	2079	-
PTP1B	50	2079	-
Transferrin Receptor	85	2052.6	-
LDLB	110	2041.27	-
p230 trans Golgi	230	2018	-
Antigen Name	Mol Wt	Signal Intensity (Brain)	Reactivity (Brain)
c-Cbl (pY700), Phospho-Specific	120	2015.5	-
TBP	37	2013.51	-
CLP-36	38	2006	-
Nestin	220	2003	-
iNOS/NOS Type II	130	1993.1	-
I $\kappa$ B $\alpha$ /MAD-3	38	1985	-
DP-1	55	1984	-
Rin1	90	1977.66	-
Smac/DIABLO	22	1947	-
TAFII135	135	1942.3	-
5-Lipoxygenase	79	1942	-
DBP2	119	1941.41	-
Bcl-x	26	1941	-
Ku-80	80	1940.72	-
CD22	140	1918.36	-
HspBP1	40	1904.73	-
DRBP76	90	1902.51	-
SLK	220/133	1884.65	-
p115	115	1884	-
Ubch7	18	1872.77	-
Jun	39	1870	-
trk B	145/95	1869	-
GADS/Mona	38	1858.02	-
Nexilin	97	1857.42	-
tyk2	135	1857	-
Plakophilin 2	100	1843	-
MCC	100	1843	-
MRP1	192	1838.83	-
TAP	70	1804.8	-
DARPP-32	32	1801	-
C-Nap1	320	1794.63	-
Plakophilin 3	87	1793.9	-
ApoM	23/26	1779	-
AIB-1	160	1766.25	-

p116Rip	125	1765	-
53BP1	345	1756.41	-
CUL-3	89	1745.37	-
Antigen Name	Mol Wt	Signal Intensity (Brain)	Reactivity (Brain)
XPF	115	1739.25	-
p120 Catenin (pY96), Phospho-Specific	120	1736.91	-
P-Akt	59	1731	-
XRCC4	55	1727	-
hPrp18	42	1726	-
Tpl-2	60	1725	-
ZNF191	48	1715.74	-
FXR2	95	1709	-
AGS3	80	1707.46	-
Ntk	56	1704.56	-
GS15	15	1702.7	-
eNOS (pS1177), Phospho-Specific	140	1697	-
Caveolin 3	18	1690.76	-
Cathepsin L	43	1686	-
CD100	150	1676	-
p21-Arc	21	1676	-
Plectin	400/500	1667	-
CapZ a	37	1658.09	-
Caspase-7/MCH-3	35	1650	-
Annexin VII	51	1649.82	-
Mint1	120	1649	-
PIP5Kg	87/90	1638	-
AIP1	105	1636	-
ICBP90	97	1632.08	-
PECI	39	1627	-
Phospholipase Cb4	130	1618	-
Casein Kinase IIb	25	1614	-
ABP-280	280	1611	-
nNOS/NOS type I	155	1595.83	-
RAP30	30	1586	-
Arc	55	1583.67	-
GBF1	206	1583	-
p140mDia	140	1581.16	-
Rap1	21	1580	-
Caveolin 1	22	1577.37	-
CRP2	23	1577	-
TOK-1	45/50	1571.34	-

Antigen Name	Mol Wt	Signal Intensity (Brain)	Reactivity (Brain)
Hck	59/56	1561	-
Topo IIa	170	1552	-
MKK3b	37	1532	-
Stat2	113	1531	-
ISGF3g	48	1528	-
IGF-IIR	273	1525	-
CBFb	22	1524	-
NKT	60	1521.92	-
p120 Catenin (pY228), Phospho-Specific	120	1518.93	-
IQGAP1	195	1517	-
iNOS/NOS Type II	130	1506.6	-
ERp72	69	1505.54	-
SLP-76	76	1505.24	-
eNOS/NOS Type III	140	1497	-
FACTp140	140	1496.04	-
Acid Ceramidase	13	1492.51	-
NuMA	238	1490.25	-
TFII-I/BAP-135	135/140	1483	-
Syntaxin 4	32	1477.15	-
GGA2	67	1475.97	-
Thrombospondin-2	200	1472.68	-
HERC2	527	1471.03	-
Bid	23	1453	-
FLAP	85	1428.44	-
Stat6 (pY641), Phospho-Specific	100	1421	-
GMAP-210/Trip230	210	1416.81	-
Paxillin	68	1410	-
Synaptogyrin	29	1401	-
GM130	130	1400	-
PI31	31	1398.44	-
Chromogranin A/CGA	86	1393	-
p38 (pT180/pY182) Phospho-Specific	42	1393	-
p42(IP4)	42	1384.36	-
CRMP5	66	1384.17	-
Sin	95	1384	-
Cip1/WAF1	21	1369	-
DAP Kinase	160	1367.37	-
Antigen Name	Mol Wt	Signal Intensity (Brain)	Reactivity (Brain)
RanBP1	29	1353.42	-
Kalinin B1	140	1344	-

Brevican	145	1325.17	-
PhLP	45	1324.73	-
MCM6	105	1320	-
Integrin $\alpha$ L/LFA-1a	180	1319.59	-
Integrin $\beta$ 3 (pY759), Phospho-Specific	104	1317.02	-
ZAP70 (pY319), Phospho-Specific	70	1315	-
ApoA-I	27	1315	-
RBP	21	1314.71	-
Headpin	44	1307.3	-
Utrophin	400	1303.27	-
Nup88	88	1299	-
Stat5A	92	1287	-
DNA Polymerase $\epsilon$ catalytic	261	1283	-
PI3-Kinase p170	170	1279.51	-
TREX1	32	1267.8	-
TRADD	34	1267.47	-
S100B	8	1250.32	-
Endopeptidase 3.4.24.16	80	1249.6	-
PKCh	82	1244.47	-
FAK (pY397), Phospho-Specific	125	1244	-
Annexin II Light Chain	11	1239	-
MGMT	25	1235.99	-
p84N5	84	1229.83	-
VAP-1	110/220	1229	-
Integrin $\alpha$ 5	150	1215.7	-
Tyro3	140	1213.91	-
NFAT-1	120	1212.61	-
hPrp16	140	1208	-
Nedd4	110	1206.69	-
BUBR1	125	1204.54	-
Arginase I	35	1200.36	-
DNA-PKcs/p350	350	1194.94	-
IGTP	48	1192.4	-
PMF-1	23	1186	-
Ick	56	1185.15	-
Antigen Name	Mol Wt	Signal Intensity (Brain)	Reactivity (Brain)
MRCKa	190	1179.49	-
Insulin Receptor b	95	1175.39	-
TCBP-49	49	1171.61	-
Ataxin-2	150	1171.41	-
CUL-1	90	1171	-
FEZ1	75	1162.78	-

Nogo-A	220	1144	-
HIF-1a	120	1130.93	-
p23	23	1129	-
Smac/DIABLO	22	1114.03	-
AKAP149	149	1108.76	-
3-Oct	46	1108	-
Exportin-t	110	1104.78	-
A-Raf	68	1103	-
PKBa/Akt	59	1094.81	-
Mitotin	357	1090.73	-
Rad50	154	1088.91	-
Zyxin	83	1086.56	-
FPTase a	48	1082.85	-
FPTase b	46	1074	-
Stat1 (pY701), Phospho-Specific	84/91	1073.5	-
Stat4	89	1069.81	-
BMPR-II	130	1067.96	-
AKAP95	95	1066.05	-
SATB1	106	1064.61	-
4F2 hc/CD98HC	80	1050.11	-
DHFR	21	1047.91	-
HIF-1b/ARNT1	95	1047.46	-
Bad	23	1043	-
Laminin B2	220	1038.06	-
Rab5ip	75	1038	-
Ndr	55	1037.66	-
Caveolin 1	22	1036	-
Villin	95	1022.75	-
mSin3A	150	1016.59	-
Endoglin	95	1007	-
Eg5	120	1006	-
Antigen Name	Mol Wt	Signal Intensity (Brain)	Reactivity (Brain)
ERK3	62	1003.86	-
E-Cadherin	120	1000.09	-
G3BP	68	996.75	-
PEX5	90	993.95	-
Sacsin	437	992	-
Bog	19	990.19	-
AKAP450	450	989	-
Frabin	105	984.48	-
HEC	76	982.33	-
MCM5	90	976.74	-

MAD2	24	976.32	-
TLP1	240/230	975.53	-
Cdk1/Cdc2	34	971.72	-
Inhibitor 2	32	968.59	-
ZPR1	51	968.26	-
Acetylcholine Receptor b	55	962.31	-
Mint3/X11g	61	960.58	-
MCAM	113	958	-
L22	15	937	-
p47phox	47	934.43	-
DLC-1	123	928.41	-
PP2Cd	48	923.32	-
Myosin Vb/Myr6	214	918.53	-
mGluR1	133	898	-
KSR-1	115	890.24	-
PIN	10	886	-
HS1	75	883	-
Caspase-3/CPP32	32	882	-
Paxillin (pY118), Phospho-Specific	68	880.73	-
AKAP220	220	875	-
NHE-3	80	865.08	-
Rab27	25	863	-
PDI	55	859.01	-
Moesin	78	857.24	-
SMRT	340	850.01	-
TAF-172	172	845.72	-
HNF-1a	92	841	-
Antigen Name	Mol Wt	Signal Intensity (Brain)	Reactivity (Brain)
GS28	28	827.55	-
KIF3B	95	827.28	-
SLK	220/133	827.21	-
PCNA	36	825.23	-
Calsarcin-2	34	812.26	-
SKAP55	55	810.55	-
MSH6/GTBP	160	791.78	-
tNASP	150	791	-
NPAT	280	787.9	-
DDX1	82	742.88	-
FYB/SLAP-130	130	739.57	-
NUDT5	40	738.29	-
Ki-67	395	704.72	-



TTF-I	140	703.47	-
Spot 14	17	679.35	-
NF-kB p65	65	671.49	-
CDC34	40	618.55	-
CoRest	66	617.61	-
Fas/CD95/APO-1	45	564.92	-
XPD	87	561.28	-
TopBP1	161	547.16	-
Complexin 2	19	547	-
IP3R-3	300	540.68	-
ZO-1	220	530.9	-
Arp3	50	521.67	-
AIM-1	41	510.87	-
LAIR-1	32	478	-
Lck (pY505), Phospho-Specific	56	458.08	-
PTP1C/SHP1	68	427.61	-
MSH3	127	285.66	-
Cdk4	33	283.65	-
TIF2	160	266.38	-
Calsarcin-1	32	139.62	-
<b>Antigen Name</b>	<b>Mol Wt</b>	<b>Signal Intensity (Brain)</b>	<b>Reactivity (Brain)</b>
LAP1	55	118.95	-
Cellugyrin	29	-284.65	-
			-
Phosphoserine/threonine			-

—Note—

## Successful Retrograde Transport of Fluorescent Latex Nanospheres in the Cerebral Cortex of the Macaque Monkey

Yuki SATO<sup>1)</sup>, Daisuke KOKETSU<sup>1)</sup>, Naohide AGEYAMA<sup>2)</sup>, Fumiko ONO<sup>2)</sup>,  
Yusei MIYAMOTO<sup>1)</sup>, and Tatsuhiko HISATSUNE<sup>1)</sup>

<sup>1)</sup>Department of Integrated Biosciences, Graduate School of Frontier Sciences, The University of Tokyo, 5-1-5 Kashiwanoha, Kashiwa-shi, Chiba 277-8562, and <sup>2)</sup>Tsukuba Primate Center for Medical Science, National Institute of Infectious Diseases, 1 Hachimandai, Tsukuba-shi, Ibaraki 305-0843, Japan

**Abstract:** Retrograde axonal transport of latex nanospheres offers a means of delivering chemical agents to a targeted region of the central nervous system (CNS). In this study we performed microinjections of latex nanospheres into the cerebral cortex of cynomolgus monkeys and observed successful retrograde labeling of neurons in the contralateral region. Our data indicate the successful use of this delivery system, reported in studies using other animals, may also be achievable with primates as well.

**Key words:** cerebral cortex, primates, retrograde transport

The retrograde targeting of projection neurons by fluorescent latex nanospheres has been used as an experimental basis for various studies. While a number of techniques exist for retrograde tract tracing to be performed, the latex nanosphere method has several unique advantages: nanospheres produce a clearly restricted region of retrograde uptake, can carry and deliver chemical agents, and are nontoxic to living cells [7, 8, 12]. These features of nanospheres have been made use of to deliver carbachol to discrete regions of the cat pontine brain stem in studies of REM sleep [16], to deliver neurotrophins to distinct populations of neurons in the cortex of ferrets [18], and to induce selective apoptotic neuronal degeneration produced by chromophore-targeted laser photolysis [11, 13, 14].

In this work, we observed the retrograde transport of

nanospheres within the monkey nervous system. Furthermore, we evaluated the possibility of applying the experimental approach of targeted apoptotic neuronal cell death, which is one of the most common ways in which the nanosphere delivery system has been employed using other animal models [2, 3, 19–21]. This was done by confirming that craniotomy and laser illumination could be performed on macaque monkeys without causing any non-specific damage. Since many reports have suggested the usefulness of the latex nanosphere delivery system (LNDS) for future therapeutic studies [4, 10, 14, 20–22], it makes sense to investigate this theme with primates in order to establish a model for performing appropriate preclinical examinations prior to using the technique on humans.

This study was carried out on one adult male and

---

(Received 17 November 2003 / Accepted 26 January 2004)

Address corresponding: T. Hisatsune, Department of Integrated Biosciences, Graduate School of Frontier Sciences, The University of Tokyo, 5-1-5 Kashiwanoha, Bioscience Bldg-402, Kashiwa-shi, Chiba 277-8562, Japan

one adult female *Macaca fascicularis* (Cynomolgus monkey; 6 and 14 years old, respectively) which were reared at the Tsukuba Primate Center. They were cared for in accordance with the Guide for the Care and Use of Laboratory Animals of the National Institute of Infectious Diseases [6] and the Guiding Principles for Animal Experiments Using Nonhuman Primates formulated by the Primate Society of Japan [17]. Experimental procedures were approved by the Graduate School of Frontier Sciences (Chiba, Japan), the University of Tokyo and the Animal Welfare and Animal Care Committee of the National Institute of Infectious Diseases (Tokyo, Japan).

The efficiency of retrograde labeling by nanospheres (Retrobeads; Lumafluor, Naples, FL) was studied by microinjecting nanospheres into the motor cortex and somatosensory cortex of monkey brains (Fig. 1). However, the experiments with the male *M. fascicularis* (*M. fascicularis* #1) revealed a problem associated with the surgical procedure. For the experiments with *M. fascicularis* #1 the dura over the microinjection sites and the contralateral region was removed in order to provide easy access to the brain. As a result, the upper layers of the experimental regions were injured traumatically by pressure from overlaying bone wax or skull and a considerable number of cells were degenerated as a consequence.

In order to overcome this technical problem, we performed the experiments with the female *M. fascicularis* (*M. fascicularis* #2) as described below. *M. fascicularis* #2 was put under isoflurane (A.D.S.1000; Shin-ei, Tokyo, Japan)-induced general anesthesia and the skull was exposed by a dorsal midline incision. A piece of bone was cut out from the skull over the left hemisphere to expose the superior frontal gyrus (SFG). The dura was not removed but rather the microinjecting needle was pushed through it and nanospheres injected into the brain using an automatic nanoliter injector (Nanoject II; Drummond Scientific Company, Broomall, PA) at depths of up to 2,000  $\mu\text{m}$  from the surface. The microinjections were made at 10 sites spaced 300  $\mu\text{m}$  apart and repeated 6 times throughout the exposed area. After completion of the microinjections, the piece of skull bone was put back in place and sealed with gelatin sponge.

Sites on the contralateral cortices homologous to the nanosphere injection sites were exposed to light from a

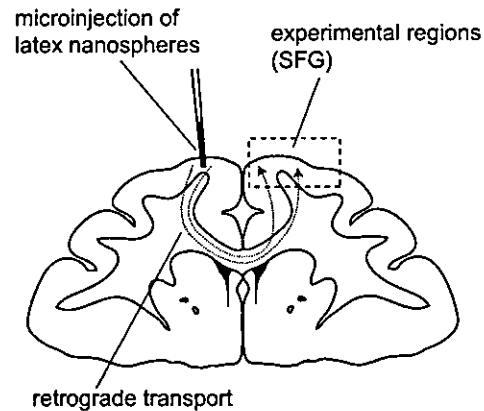
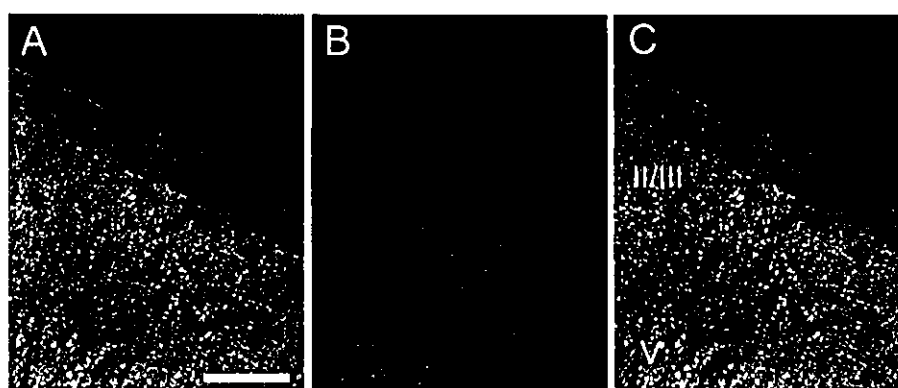


Fig. 1. Schematic representation of retrograde targeting of projection neurons by fluorescent latex nanospheres in the macaque cerebral cortex. Nanospheres microinjected into the left hemisphere were callosally transported to the homologous region of the right hemisphere.

laser (Schäfter + Kirchhoff GmbH, Hamburg, Germany) 35 days after the microinjections. The wave length of the laser light was set to 674 nm, which is the same as that used in experiments investigating targeted apoptotic neuronal cell death [11, 13]. To accomplish this, the animal was placed under general anesthesia (A.D.S.1000; Shin-ei) with isoflurane gas and a piece of skull over the experimental region was removed to expose the motor and somatosensory cortices of the right hemisphere. The dura was left intact. The experimental region was then exposed to laser light, yielding a total incident energy density of approximately 5,700 J/cm<sup>2</sup>. After the laser illumination, the piece of skull was put back in place and sealed with gelatin sponge.

Twenty-eight days after laser illumination, *M. fascicularis* #2 was sacrificed under general anesthesia by administration of ketamine hydrochloride (Ketalar, 10 mg/kg; Sankyo, Tokyo, Japan) and xylazine hydrochloride (Seraktar, 0.5 mg/kg; Bayer, Leverkusen, Germany) transcardially perfused with phosphate-buffered saline (PBS), followed by 4% paraformaldehyde (PFA). The removed brain was dissected into right and left hemispheres. Each hemisphere was cut into blocks of side-length 5 mm, postfixed for 2 days at 4°C in fresh 4% PFA, and cryoprotected by infiltration with 30% sucrose in PBS for 3 days. The brain blocks were put into O.C.T. compound (Sakura, Tokyo, Japan) and



**Fig. 2.** Distribution of transported nanospheres in cerebral cortex. *A*, Nissl staining of neurons with NeuroTrace (green). *B*, Fluorescent nanospheres can be seen in red. *C*, Merged overlay of *A* and *B* indicating that the nanospheres are present specifically in layers II/III and V. Scale bar = 300  $\mu$ m.

frozen at  $-80^{\circ}\text{C}$ . The specimens were then coronally sectioned with a cryostat (MICROM, Walldorf, Germany) at a thickness of 50  $\mu$ m and preserved in a cryoprotectant solution (30% ethylene glycol, 30% glycerol in 0.05 M phosphate buffer) or 0.1% sodium azide in PBS until they were processed.

Brain sections were stained with NeuroTrace green fluorescent Nissl stain (1:50; Molecular Probes, Eugene, OR). The sections were washed with PBS and placed on poly-L-lysine-coated glass slides. They were then treated with 0.1% Triton X-100 in PBS and incubated with the stain solution for 10 min. After washing with PBS, GelMount was applied and the sections were coverslipped. In addition to the above, the sections were also stained immunohistochemically for NeuN, GFAP and BrdU and examined using a confocal laser scanning microscope (TCS SP2; Leica, Wetzlar, Germany), with analysis performed using three-dimensional (3D) image processing software (LSC; Leica) as previously described [9].

Layer construction and the distribution of neurons in the contralateral regions were visualized by Nissl staining with NeuroTrace, and the widespread and clear transportation of the nanospheres was confirmed (Fig. 2A–C). Here, we focused our investigations on the SFG of the right hemisphere, which was exactly contralateral to the microinjection sites, because the transported nanospheres aggregated predominantly in this region. In some areas of the region, nanospheres were present specifically in neocortical layers II/III and

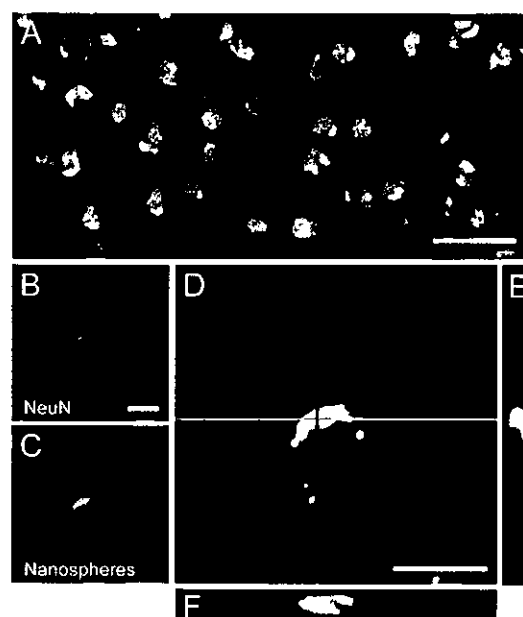


**Fig. 3.** Presence of fluorochrome carried by the transported nanospheres in NeuN-positive projection neurons. *A*, Merged overlay of images for nanosphere fluorescence (red) and immunohistochemical labeling for the mature neuronal marker NeuN (green) in layers II/III of experimental cortex. *B–F*, High magnification image of a pyramidal neuron double-labeled with NeuN (green) and nanosphere fluorescence (red). *B*, NeuN. *C*, Nanosphere fluorescence. *D*, Overlay of *B* and *C*. *E*, Cross sectional image of the purple line of *D*. *F*, Cross sectional image of the gray line of *D*. Scale bar, 50  $\mu$ m in *A*, 10  $\mu$ m in *B* and *C*, 15  $\mu$ m in *D*, *E* and *F*.

V as seen in the figure, but in other areas they were present in all layers. Although further neuroanatomical studies are necessary to provide a definitive reason for this phenomenon, we suggest that this might be because the nanospheres were microinjected into the SFG in general, rather than into a more restricted area. In this way, the nanospheres present in different layers may have originated from different regions in the injected cortex.

Given that the sections were stained with NeuN, we investigated the presence of nanospheres within neurons (Fig. 3A–F). The merged image for the nanosphere fluorescence and NeuN staining (Fig. 3A) shows that most projecting neurons in the region contain nanospheres in their somata. Only a small percentage of nanospheres were identified to be present outside of the somata, and these we believe were present in neuronal processes or in cells undergoing natural degeneration. Prior to performing the experiments, we were concerned about the issue of the distance of neuronal projection. Even though previous studies have reported that 2 weeks should be allowed to label somata in the contralateral hemisphere by retrograde transport through callosal projections in the rodent nervous system [12, 13, 20], it was not possible to know how long it would take in the nervous system of the cynomolgus monkey because the brain of primates are so large compared with brains of other mammals used formerly. However, considering the abundant distribution of nanospheres that belonged to NeuN-positive neurons, the time between microinjection and sacrifice (63 days) was more than enough for retrograde labeling of the cells to take place, although the minimum time for targeting is still unknown.

To confirm that the craniotomy and laser illumination did not lead to any non-specific damage to the experimental regions, we investigated the sections double-stained with GFAP and BrdU (data not shown). Because alterations to immunophenotype and proliferative activity of astrocytes have been observed in many brain pathologies [1, 5, 15], the number of GFAP- or BrdU-positive cells should increase if there was any significant damage. In the experimental regions, however, no augmentation of these markers was observed. These data imply that LNDS can be applied without

causing non-specific cortical damage to the macaque cerebral cortex.

The results presented in this paper suggest that the successful use of LNDS reported in various studies using different species of mammals can also be achieved with primates if the experimental conditions are carefully controlled.

## References

1. Dihné, M., Block, F., Korr, H., and Töpper, R. 2001. *Brain Res.* 902: 178–189.
2. Eyding, D., Macklis, J.D., Neubacher, U., Funke, K., and Wörgötter, F. 2003. *J. Neurosci.* 23: 7021–7033.
3. Fricker-Gates, R.A., Shin, J.J., Tai, C.C., Catapano, L.A., and Macklis, J.D. 2002. *J. Neurosci.* 22: 4045–4056.
4. Häfeli, U.O., Sweeney, S.M., Beresford, B.A., Humm, J.L., and Macklis, R.M. 1995. *Nucl. Med. Biol.* 22: 147–155.
5. Hill-Felberg, S.J., McIntosh, T.K., Oliver, D.L., Raghupathi, R., and Barbarese, E. 1999. *J. Neurosci. Res.* 57: 271–279.
6. Honjo, S. 1985. *J. Med. Primatol.* 14: 75–89.
7. Katz, J.C., Burkhalter, A., and Dreyer, W.J. 1984. *Nature* 310: 498–500.
8. Köbber, C., Apps, R., Bechmann, I., Lanciego, J.L., Mey, J., and Thanos, S. 2000. *Prog. Neurobiol.* 62: 327–351.
9. Koketsu, D., Mikami, A., Miyamoto, Y., and Hisatsune, T. 2003. *J. Neurosci.* 23: 937–942.
10. Leavitt, B.R., Hernit-Grant, C.S., and Macklis, J.D. 1999. *Exp. Neurol.* 157: 43–57.
11. Macklis, J.D. 1993. *J. Neurosci.* 13: 3848–3863.
12. Madison, R., Macklis, J.D., and Thies, C. 1990. *Brain Res.* 522: 90–98.
13. Madison, R. and Macklis, J.D. 1993. *Exp. Neurol.* 121: 153–159.
14. Magavi, S.S., Leavitt, B.R., and Macklis, J.D. 2000. *Nature.* 405: 951–955.
15. Norton, W.T. 1999. *Neurochem. Res.* 24: 213–218.
16. Quattrocchi, J.J., Mamelak, A.N., Madison, R.D., Macklis, J.D., and Hobson, J.A. 1989. *Science.* 245: 984–986.
17. Primate Society of Japan. 1986. *Primate Res.* 2: 111–113.
18. Riddle, D.R., Katz, L.C., and Lo, D.C. 1997. *BioTechniques.* 23: 928–937.
19. Scharff, C., Kirn, J.R., Grossman, M., Macklis, J.D., and Nottebohm, F. 2000. *Neuron.* 25: 481–492.
20. Sheen, V.L. and Macklis, J.D. 1995. *J. Neurosci.* 15: 8378–8392.
21. Shin, J.J., Fricker-Gates, R.A., Perez, F.A., Leavitt, B.R., Zurakowski, D., and Macklis, J.D. 2000. *J. Neurosci.* 20: 7404–7416.
22. Snyder, E.Y., Yoon, C., Flax, J.D., and Macklis, J.D. 1997. *Proc. Natl. Acad. Sci. USA.* 94: 11663–11668.

# RESEARCH ARTICLE

## Postischemic administration of Sendai virus vector carrying neurotrophic factor genes prevents delayed neuronal death in gerbils

M Shirakura<sup>1,2</sup>, M Inoue<sup>1</sup>, S Fujikawa<sup>1</sup>, K Washizawa<sup>1</sup>, S Komaba<sup>1</sup>, M Maeda<sup>3</sup>, K Watabe<sup>4</sup>, Y Yoshikawa<sup>2</sup> and M Hasegawa<sup>1</sup>

<sup>1</sup>DNAVEC Research Inc., Tsukuba, Japan; <sup>2</sup>Department of Biomedical Science, Graduate School of Agricultural and Life Sciences, University of Tokyo, Tokyo, Japan; <sup>3</sup>First Department of Anatomy, Osaka City University Medical School, Osaka, Japan; and <sup>4</sup>Department of Molecular Neuropathology, Tokyo Metropolitan Institute for Neuroscience, Tokyo, Japan

Sendai virus (SeV) vector-mediated gene delivery of glial cell line-derived neurotrophic factor (GDNF) and nerve growth factor (NGF) prevented the delayed neuronal death induced by transient global ischemia in gerbils, even when the vector was administered several hours after ischemia. Intraventricular administration of SeV vector directed high-level expression of the vector-encoded neurotrophic factor genes, which are potent candidates for the treatment of neurodegenerative diseases. After occlusion of the bilateral carotid arteries of gerbils, SeV vector carrying GDNF (SeV/GDNF), NGF (SeV/NGF), brain-derived neurotrophic factor (SeV/BDNF), insulin-like growth factor-1 (SeV/IGF-1) or vascular endothelial growth factor (SeV/VEGF) was injected into the

lateral ventricle. Administration of SeV/GDNF, SeV/NGF or SeV/BDNF 30 min after the ischemic insult effectively prevented the delayed neuronal death of the hippocampal CA1 pyramidal neurons. Furthermore, the administration of SeV/GDNF or SeV/NGF as late as 4 or 6 h after the ischemic insult also prevented the death of these neurons. These results indicate that SeV vector-mediated gene transfer of neurotrophic factors has high therapeutic potency for preventing the delayed neuronal death induced by transient global ischemia, and provides an approach for gene therapy of stroke.

Gene Therapy (2004) 11, 784–790. doi:10.1038/sj.gt.3302224  
Published online 12 February 2004

**Keywords:** Sendai virus; cerebral ischemia; delayed neuronal death; GDNF; NGF

Neurons are postmitotic and highly differentiated, and are extremely vulnerable to ischemic injury. Pyramidal cells of the hippocampal CA1 region are well known to be especially vulnerable to cerebral ischemia.<sup>1,2</sup> Neuronal cell death in the CA1 region itself is not death-dealing but results in severe deficits of memory function.<sup>3–5</sup> Since the regeneration of neuronal cells remains critically difficult at present, protection against the neuronal loss induced by ischemic injury is vital in cerebrovascular-type dementia.

Glial cell line-derived neurotrophic factor (GDNF) is a potent neurotrophic factor that promotes the cell survival and differentiation of dopaminergic neurons<sup>6,7</sup> and motoneurons.<sup>8,9</sup> Nerve growth factor (NGF) also has a potent ability to protect neurons from various injuries and promote the survival of cholinergic neurons.<sup>10–12</sup> These neurotrophic factors may be valuable as candidates for use in therapy of neurodegenerative diseases. It has been reported that the neuronal cell death induced by ischemic injury was prevented by the administration of GDNF<sup>13–15</sup> and NGF<sup>16–18</sup> proteins. However, the usefulness of such protein factors in patients is limited because of their poor bioavailability and short half-lives.

Moreover, these agents might be ineffective without direct injection and continuous infusion into the ventricle, striatum or cerebral cortex. Therefore, virus vector-mediated gene transfer is expected to be an effective approach for the delivery of therapeutic proteins into the central nervous system (CNS). Even in the case of unsustained, but transient, expression by the vectors, it would enable significant cutting down of the number of required administrations. Previous studies demonstrated that gene transfer of neurotrophic factors such as GDNF<sup>19</sup> and NGF<sup>20,21</sup> rescued neuronal cells from ischemic injury in animal models. However, there have not been any reports in which neurotrophic factors expressed using conventional vectors such as adenovirus, retrovirus or adeno-associated virus were shown to promote the survival of neurons when the vectors were administered after ischemia.

We have developed a new type of gene transfer vector using Sendai virus (SeV), which is classified as a type I parainfluenza virus belonging to the family *Paramyxoviridae* with a negative-strand RNA genome.<sup>22,23</sup> SeV has a strictly cytoplasmic life cycle in mammalian cells, that is, its genomic RNA is restricted to the cytoplasm and has no interaction with the host chromosomes.<sup>22</sup> Therefore, SeV vector causes no genotoxicity such as the permanent integration in the target cells sometimes observed with other conventional viral

Correspondence: M Inoue, 1-25-11 Kannondai, Tsukuba-shi, Ibaraki 305-0856, Japan

Received 16 May 2003; accepted 29 November 2003; published online 12 February 2004

vectors. SeV has the ability to infect most mammalian cells such as neuronal and muscular cells and directs high-level gene expression in these cells.<sup>23–26</sup> Indeed, we observed potent infectivity of SeV vector in ependymal cells after intraventricular administration in the CNS.<sup>27</sup> When the SeV vector carrying enhanced green fluorescent protein gene (SeV/GFP) was administered into the left lateral ventricle of gerbils, intense GFP expression was observed around the ependymal layer of the lateral ventricles (Figure 1c) and around the hippocampus (Figure 1b). Immunohistochemical analysis using anti-SeV antibody clearly showed that the cells supporting SeV replication were ependymal cells in the lateral ventricles (Figure 1d), third ventricle (Figure 1e) and around the hippocampus (Figure 1f). We previously showed that SeV vector-mediated gene transfer of GDNF 4 days before transient ischemia prevented the delayed neuronal death induced by transient global ischemia in gerbils.<sup>27</sup> However, SeV vector was administered prior to the ischemic insult in that case, too, whereas gene therapy must be applied after the occurrence of a stroke for clinical application. In the present study, we examined the effects of postischemic administration of SeV vectors carrying GDNF, NGF and other neurotrophic factor genes on the delayed neuronal death induced by transient global ischemia. Our results suggest that SeV vector-mediated gene transfer has a therapeutic high potential for cerebral ischemia.

In order to confirm the efficient gene transfer and expression of SeV in the CNS, the proteins derived from the genes harbored in the SeV vector were quantified. SeV vectors such as SeV/GDNF, SeV/NGF and SeV/GFP were administered into the left lateral ventricle of gerbils at  $5 \times 10^6$  PFU/head, and the amount of GDNF and NGF proteins in the hippocampus was quantified by ELISA assays. High-level expression of GDNF ( $114 \pm 6$  pg/mg tissue) and NGF ( $1130 \pm 60$  pg/mg tissue) proteins was detected in the hippocampus of gerbils as early as 1 day after injection of SeV/GDNF and SeV/NGF, respectively (Figure 2a, b). In contrast, only a very small amount of GDNF or NGF protein was detected when the gerbils were treated with SeV/GFP. The expression of GDNF ( $2340 \pm 200$  pg/mg tissue) and NGF ( $3360 \pm 290$  pg/mg tissue) proteins reached peak levels 4 days after injection of SeV/GDNF and SeV/NGF, respectively, and then returned to the original level 14 days after the injection. In another experiment, an increment of GDNF expression in the cerebrospinal fluid was detected 8 h after injection of SeV/GDNF (data not shown). These results indicate that rapid and high-level expression of neurotrophic factors can be achieved by the administration of SeV vectors in the CNS. Also, the expression level achieved using SeV vectors was remarkably high compared with that achieved using adenovirus. For example, the GDNF concentration was reported to be  $2.2 \pm 0.5$  pg/mg tissue 1 day after the

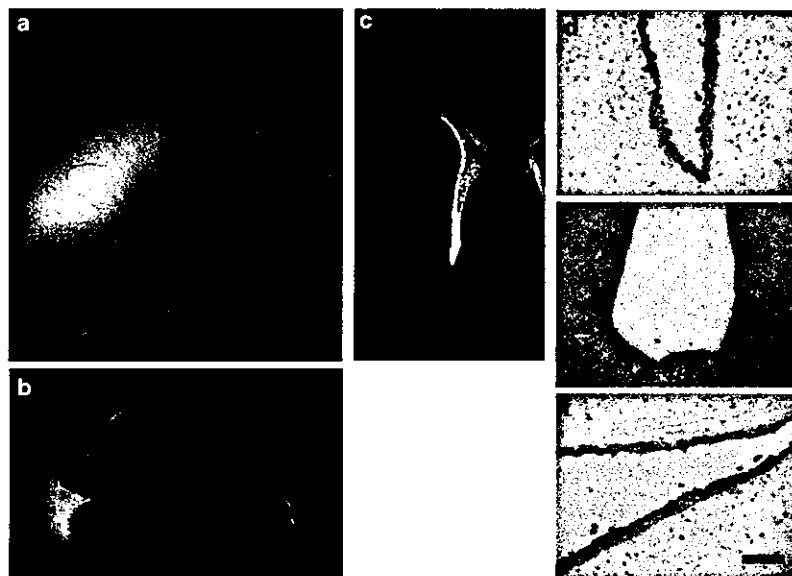


**Figure 1** Identification of cell types supporting SeV replication. SeV vector carrying GFP gene (SeV/GFP;  $5 \times 10^6$  PFU/head) was injected into the left lateral ventricle of gerbils as described previously,<sup>27</sup> and the GFP expression 4 days after the injection was observed under a stereoscopic fluorescence microscope (Leica, Germany) from the surface of the top of brain (a) and with coronal sections around the hippocampus (b) and lateral ventricle (c). For the coronal sections, the brain was sliced into 300- $\mu$ m-thick slices with a microslicer (DTK-1000; Dosaka, Japan). Representative photographs of immunohistochemical staining for SeV are shown (d–f). The paraffin sections were pretreated with 0.3%  $H_2O_2$  in PBS, followed by washing thrice. After blocking with 10% normal goat serum (NGS) in PBS for 1 h, the sections were incubated overnight at 4°C with a rabbit polyclonal antibody to SeV (anti-SeV)<sup>28</sup> in 3% NGS and 0.3% Triton X-100 in PBS. The sections were then washed and incubated for 1 h with biotinylated anti-rabbit IgG (Vector Laboratories, Burlingame, CA, USA), followed by incubation for 1 h with the reagents for avidin-biotin complex formation (Vector Laboratories). Immunopositive cells were visualized by reaction with 3,3'-diaminobenzidine tetrahydrochloride (DAB) (WAKO Pure Chemicals, Tokyo, Japan) and counterstained with hematoxylin. Scale bars = 100  $\mu$ m. The ependymal cells along the (d) lateral ventricle, (e) third ventricle and (f) hippocampus were SeV positive.

injection into the cortex of adenovirus ( $1 \times 10^8$  PFU/head) carrying the GDNF gene.<sup>29</sup>

We next examined the effects of the postischemic administration of SeV vectors on the delayed neuronal death of the hippocampal CA1 pyramidal cells induced by transient ischemia. It has been reported that the direct administration of the bcl-2 gene mediated by adenovirus (AAV) into pyramidal neurons within 1 h after ischemic insult prevents the delayed neuronal death in gerbils.<sup>30</sup> However, direct injection of virus vectors into the cerebral parenchyma cells, especially in

the hippocampus, is more invasive than intraventricular administration. Therefore, we selected a single intraventricular administration and utilized SeV-transduced ependymal cells to produce proteins from the genes carried by the vectors.<sup>27</sup> Accordingly, SeV/GDNF and SeV/NGF ( $5 \times 10^6$  PFU/head) were injected into the lateral ventricles of ischemic gerbils after 30 min of occlusion of the bilateral carotid arteries, and histopathological analysis was conducted 6 days after the injection. The effects of the above vectors were compared with those of SeV vectors carrying brain-derived neurotrophic factor (SeV/BDNF), insulin-like growth factor-1 (SeV/IGF-1) and vascular endothelial growth factor (SeV/VEGF). All the genes carried by the vectors have been reported to prevent neuronal degeneration after transient ischemia,<sup>31–33</sup> and for each SeV vector, vector-derived expression in infected cells was confirmed *in vitro* (data not shown). In sham-operated gerbils, surviving wheel-like nuclei were observed in the pyramidal cells in CA1 (Figure 3a). However, in gerbils treated with SeV/GFP, almost all of the pyramidal cells in the hippocampal CA1 region showed pyknotic degenerative nuclei in the pyramidal cells (Figure 3g). In contrast, treatment of gerbils with SeV/GDNF or SeV/NGF ameliorated the delayed neuronal death in the hippocampal CA1 pyramidal cells (Figure 3b, c). Treatment with SeV/BDNF also showed ameliorative effects (Figure 3d), but treatment with SeV/VEGF did not (Figure 3f). Treatment with SeV/IGF-1 showed ameliorative effects (Figure 3e) in only two gerbils among eight tested. For quantitative analysis, the number of surviving neurons/1-mm length in the hippocampal CA1 region was counted (Figure 4). Treatment with SeV/GDNF ( $180.8 \pm 11.7$  cells/mm) or SeV/NGF ( $142.4 \pm 24.3$  cells/mm) significantly prevented neuronal death as compared to treatment with SeV/GFP ( $10.7 \pm 1.9$  cells/mm) ( $P < 0.01$ ). Treatment with SeV/BDNF ( $139.3 \pm 29.7$  cells/mm) also reduced the cell death of the neurons by about 70%. SeV/GDNF and SeV/NGF (and SeV/BDNF) proved to be better for the treatment of transient global ischemia than SeV vectors carrying genes for the other factors investigated here. As a way to confirm that the vector-derived growth factors actually increased and acted to prevent the neuronal death of the hippocampal CA1 pyramidal neurons, we measured the concentrations of both NGF and GDNF proteins in the hippocampus of 'ischemic' gerbils 4 days after the injection of SeV/GDNF or SeV/NGF into the lateral ventricle. When the SeV/GDNF was injected at 4 h after ischemia, the concentration of GDNF ( $71.9 \pm 12.0$  pg/mg tissue) was increased compared to that of SeV/GFP-injected ( $0.057 \pm 0.022$  g/mg tissue) or untreated ( $0.038 \pm 0.042$  pg/mg tissue) gerbils. However, the concentration of NGF ( $15.8 \pm 0.9$  pg/mg tissue) remained at the original level of SeV/GFP-injected ( $15.4 \pm 4.6$  pg/mg tissue) or untreated ( $18.2 \pm 6.2$  pg/mg tissue) gerbils. When the SeV/NGF was injected at 4 h after ischemia, the concentration of NGF ( $1570 \pm 210$  pg/mg tissue) but not that of GDNF ( $0.074 \pm 0.047$  pg/mg tissue) increased, and this NGF could show a neuroprotective effect. These results indicate that the vector-derived growth factors rather than the intrinsic ones increase and function to prevent the neuronal death.

To examine the effect of extending the time until the administration of SeV vectors after ischemic insult, which is important for practical use in clinical applications,

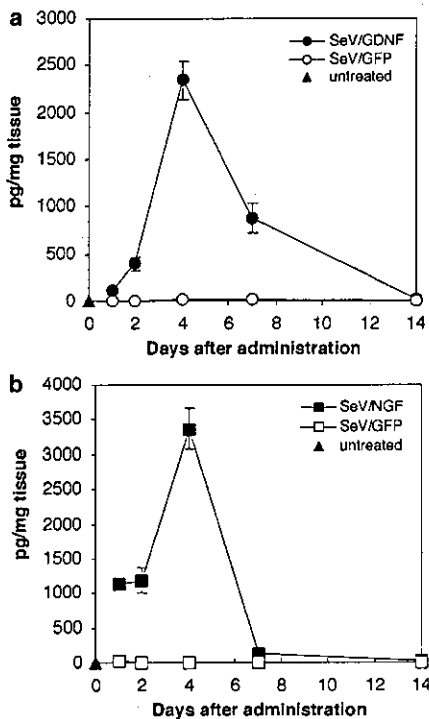


**Figure 2** Kinetics of the expression of GDNF and NGF proteins in the hippocampus. Gerbils were injected with SeV vectors carrying GDNF (SeV/GDNF), NGF (SeV/NGF) or GFP (SeV/GFP) genes ( $5 \times 10^6$  PFU/head,  $n=20$  animals per group) into the left lateral ventricle as described.<sup>27</sup> At 1, 2, 4, 7 or 14 days after the injection, the concentrations of GDNF and NGF in the hippocampus were measured using ELISA kits (Promega, WI, USA) as previously described.<sup>27</sup> The hippocampus was harvested from four gerbils at each time point. SeV/GDNF and SeV/GFP were constructed as previously described.<sup>27</sup> SeV/NGF was constructed as described.<sup>27,28</sup> Briefly, mouse NGF (accession number: M14805) cDNA was amplified with a pair of NotI-tagged (underlined) primers containing SeV-specific transcriptional regulatory signal sequences, 5'-ACTTG CGGCCGCGCCAAAGTTCAGTAATGTCCATGTTGTTCTACACTCTG-3' and 5'-ATCCGCGCGCCGCGATGAACCTTCACCCCTAAGTTTCTTCTACGGTCAGCCTCTTCTGTAGCCTTCCTGC-3'. The amplified fragment was introduced into the NotI site of the parental pSeV18<sup>+</sup>(+), which was constructed to produce the exact SeV full-length antigenomic RNA, to generate pSeV/NGF. pSeV/NGF was transfected into LLC-MK<sub>2</sub> cells after infection of the cells with vaccinia virus vTF7-3, which expresses T7 polymerase. The T7-driven full-length recombinant SeV/NGF RNA genomes were encapsulated by NP, P and L proteins, which were derived from the respective cotransfected plasmids. After incubation for 40 h, cell lysates of transfected cells were injected into embryonated chicken eggs to amplify the recovered viruses. The virus titers were determined using a hemagglutination units (HAU) assay. Values are expressed as the mean  $\pm$  s.d.



Genotype	Survival (cells/mm)	Significance
sham	~215	
SeVGDNF	~185	*
SeVNGF	~145	*
SeVBDNF	~145	*
SeVIGF1	~50	
SeVVEGF	~10	
SeVIGF2	~10	

## Gene Therapy

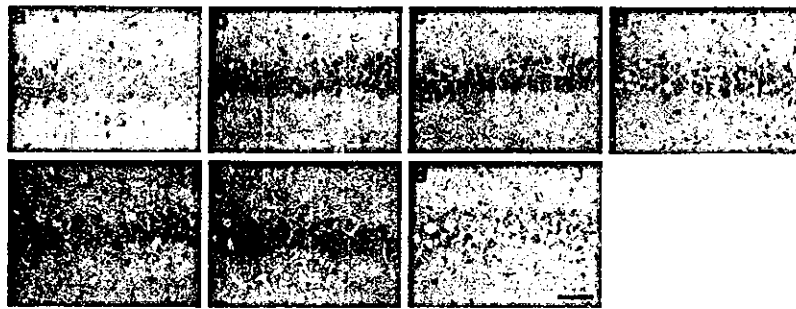


**Figure 5** Representative photographs of pyramidal neurons in the hippocampal CA1 regions after treatment (4 and 6 h after ischemia) with SeV vector following ischemic injury. SeV/GDNF (b, e), SeV/NGF (c, f) or SeV/GFP (d, g) was administered intraventricularly 4 h (b, c, d) or 6 h (e, f, g) after ischemic insult. The sections were stained with hematoxylin and eosin. Scale bar = 50  $\mu$ m. Occlusion of the bilateral common carotid arteries was performed as described in Figure 2.

neuronal death of the hippocampal CA1 pyramidal neurons induced by transient ischemia. Moreover, these attractive features of SeV vectors may make them useful for the treatment of acute diseases such as cerebral ischemia.

It has been reported that NGF administration prevented the delayed neuronal death when neurons were observed 7 days after ischemic insult, but not when they were observed 28 days after the insult.<sup>18</sup> The long-term effects of the vectors studied here therefore had to be examined to better clarify their potential benefits in clinical use. Therefore, we also examined the long-term effects of SeV/GDNF and SeV/NGF on delayed neuronal death. The effect of SeV vectors for preventing neuronal death could be observed even when analyzed 28 days after the insult, although it was not seen in the case of topical application of NGF protein.<sup>18</sup> However, the number of surviving neurons at 28 days after the ischemia was reduced to almost half of that at 6 days after ischemia in the cases of gerbils treated with SeV/GDNF and SeV/NGF (Figure 7). High-level expression of the vector-encoded protein was detected after the administration of the SeV vector, but this expression reached a peak 4 days after the administration and then decreased to the basal level by 14 days. It is probable that immune responses induced by the virus particles or genes derived from SeV may cause the rapid decline of the gene expression of SeV. However, this limitation may be circumvented by the development of a new generation of SeV vectors that elicit weaker immune responses, which should extend the duration of gene expression. We have developed a series of an attenuated type of SeV vectors that are F gene-deleted,<sup>24</sup> F gene-deleted with preferable mutations,<sup>35</sup> M gene-deleted,<sup>36</sup> or have combinations of deletions of these genes (Kitazato K, unpublished; Inoue M, unpublished). We plan the first clinical application of SeV vector carrying human fibroblast growth factor-2 for the treatment of peripheral arterial disease using F gene-deleted SeV vector. As the F gene-deleted SeV is nontransmissible and shows less cytopathic effect than the wild-type SeV, we should utilize this type of SeV (or further advanced types of SeV vector) for applications to brain ischemia. Improvement of the vector modifications will ultimately provide better protection against ischemic injury. Moreover, alternative administration routes, such as lumbar puncture of the vectors, should be developed for the purposes of human

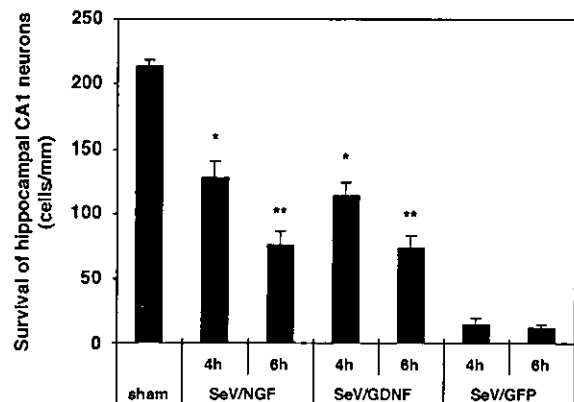


**Figure 6** Quantitative analysis of the effect of SeV vector on ischemic injury when administered 4 and 6 h after ischemia. SeV/GDNF, SeV/NGF or SeV/GFP was injected intraventricularly 4 or 6 h after ischemic insult. The number of surviving neurons/1-mm length in the hippocampal CA1 region was calculated. Values are expressed as the mean  $\pm$  s.d. ( $n=8$  animals per group). Asterisks indicate a significant difference as compared with the SeV/GFP-treated group. ( $P<0.01$ , Student's  $t$  test).

gene therapy for cerebrovascular diseases. Hayashi and co-workers<sup>37</sup> reported that liposome-mediated hepatocyte growth factor (HGF) gene transfer into the subarachnoid space prevented delayed neuronal death in gerbils. Intrathecal injection into the cisterna magna involves no systematic anesthesia, no burr hole and no pain for patients. For use in clinical application, these methods should be tested in future studies. More importantly, we have already confirmed the efficient replication of SeV vectors in primates. In fact, high-level expression of GDNF (more than 100 ng/ml) was observed in cerebrospinal fluid after the injection of SeV vector carrying the GDNF gene (SeV/GDNF) into the lateral ventricle of primates (data not shown). Thus, we are going to evaluate the SeV/GDNF vector for its effects on the recovery from brain ischemia using primates. In such experiments, we hope to show a correlation between CA1 neuroprotection and functional recovery.

In conclusion, the present study demonstrated that postischemic administration of SeV vectors carrying genes for GDNF and NGF effectively prevented the delayed neuronal death of the hippocampal CA1

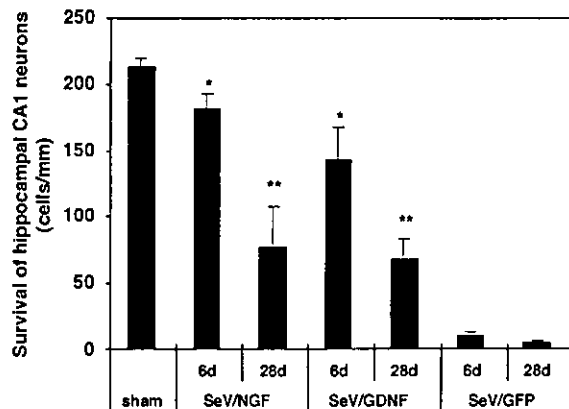


Figure 7 Long-term effect of the SeV vectors on ischemic injury. SeV/GDNF, SeV/NGF or SeV/GFP was injected intraventricularly 30 min after ischemic insult. At 6 days or 28 days after injection, gerbils were anesthetized, and the number of surviving neurons/1-mm length in the hippocampal CA1 region was calculated. Values are expressed as the mean  $\pm$  s.d. ( $n=8$  animals per group). Asterisks indicate a significant difference as compared with the SeV/GFP-treated group. ( $P<0.01$ , Student's  $t$  test).

pyramidal cells induced by occlusion of the bilateral carotid arteries. It is noteworthy that the neuroprotective effect was obtained even 4 and 6 h after ischemic insults. These results indicate that gene therapy using SeV vectors is of great potential usefulness for the treatment of cerebral ischemia.

### Acknowledgements

We thank T Yamamoto for technical assistance, and A Iida, M Okayama and M Fukumura for helpful discussions.

### References

- 1 Kirino T. Delayed neuronal death in the gerbil hippocampus following ischemia. *Brain Res* 1982; 239: 57–59.
- 2 Kirino T, Sano K. Selective vulnerability in the gerbil hippocampus following transient ischemia. *Acta Neuropathol (Berl.)* 1984; 62: 201–208.
- 3 Andersen MB, Sams-Dodd F. Impairment of working memory in the T-maze after transient global cerebral ischemia in the Mongolian gerbil. *Behav Brain Res* 1998; 91: 15–22.
- 4 Li AJ et al. Protective effect of acidic fibroblast growth factor against ischemia-induced learning and memory deficits in two tasks in gerbils. *Physiol Behav* 1999; 66: 577–583.
- 5 Catania MA et al. Erythropoietin prevents cognition impairment induced by transient brain ischemia in gerbils. *Eur J Pharmacol* 2002; 437: 147–150.
- 6 Beck KD et al. Mesencephalic dopaminergic neurons protected by GDNF from axotomy-induced degeneration in the adult brain. *Nature* 1995; 373: 339–341.
- 7 Choi-Lundberg DL et al. Dopaminergic neurons protected from degeneration by GDNF gene therapy. *Science* 1997; 275: 838–841.
- 8 Henderson CE et al. GDNF: a potent survival factor for motoneurons present in peripheral nerve and muscle. *Science* 1994; 266: 1062–1064.
- 9 Li L et al. Rescue of adult mouse motoneurons from injury-induced cell death by glial cell line-derived neurotrophic factor. *Proc Natl Acad Sci USA* 1995; 92: 9771–9775.
- 10 Fischer W et al. Amelioration of cholinergic neuron atrophy and spatial memory impairment in aged rats by nerve growth factor. *Nature* 1987; 329: 65–68.
- 11 Montero CN, Hefti F. Rescue of lesioned septal cholinergic neurons by nerve growth factor: specificity and requirement for chronic treatment. *J Neurosci* 1988; 8: 2986–2999.
- 12 Tuszynski MH, U HS, Amaral DG, Gage FH. Nerve growth factor infusion in the primate brain reduces lesion-induced cholinergic neuronal degeneration. *J Neurosci* 1990; 10: 3604–3614.
- 13 Abe K, Hayashi T, Itoyama Y. Amelioration of brain edema by topical application of glial cell line-derived neurotrophic factor in reperfused rat brain. *Neurosci Lett* 1997; 231: 37–40.
- 14 Kitagawa H et al. Reduction of ischemic brain injury by topical application of glial cell line-derived neurotrophic factor after permanent middle cerebral artery occlusion in rats. *Stroke* 1998; 29: 1417–1422.
- 15 Miyazaki H et al. Glial cell line-derived neurotrophic factor protects against delayed neuronal death after transient forebrain ischemia in rats. *Neuroscience* 1999; 89: 643–647.
- 16 Shigeno T et al. Amelioration of delayed neuronal death in the hippocampus by nerve growth factor. *J Neurosci* 1991; 11: 2914–2919.
- 17 Yamamoto S et al. Protective effect of NGF atelocollagen mini-pellet on the hippocampal delayed neuronal death in gerbils. *Neurosci Lett* 1992; 141: 161–165.
- 18 Ishimaru H et al. NGF delays rather than prevents the cholinergic terminal damage and delayed neuronal death in the hippocampus after ischemia. *Brain Res* 1998; 789: 194–200.
- 19 Yagi T et al. Rescue of ischemic brain injury by adenoviral gene transfer of glial cell line-derived neurotrophic factor after transient global ischemia in gerbils. *Brain Res* 2000; 885: 273–282.
- 20 Hermann DM et al. Adenovirus-mediated GDNF and CNTF pretreatment protects against striatal injury following transient middle cerebral artery occlusion in mice. *Neurobiol Dis* 2001; 8: 655–666.
- 21 Andsberg G et al. Neuropathological and behavioral consequences of adeno-associated viral vector-mediated continuous intrastriatal neurotrophin delivery in a focal ischemia model in rats. *Neurobiol Dis* 2002; 9: 187–204.
- 22 Lamb RA, Kolakofsky D. Paramyxoviridae: the virus and their replication. In: Fields BN, Knipe DM, Howley PM (eds) *Fields Virology*. Lippincott-Raven: Philadelphia, 1996, pp. 1177–1204.
- 23 Nagai Y, Kato A. Paramyxovirus reverses genetics is coming of age. *Microbiol Immunol* 1999; 43: 613–624.
- 24 Li HO et al. A cytoplasmic RNA vector derived from non-transmissible Sendai virus with efficient gene transfer and expression. *J Virol* 2000; 74: 6564–6569.
- 25 Yonemitsu Y et al. Efficient gene transfer to airway epithelium using recombinant Sendai virus. *Nat Biotechnol* 2000; 18: 970–973.
- 26 Shiotani A et al. Skeletal muscle regeneration after insulin-like growth factor I gene transfer by recombinant Sendai virus vector. *Gene Therapy* 2001; 8: 1043–1050.
- 27 Shirakura M et al. Sendai virus vector-mediated gene transfer of glial cell line-derived neurotrophic factor prevents delayed neuronal death after transient global ischemia in gerbils. *Exp Anim* 2003; 52: 119–127.
- 28 Kato A et al. Initiation of Sendai virus multiplication from transfected cDNA or RNA with negative or positive sense. *Genes Cells* 1996; 1: 569–579.
- 29 Kitagawa H et al. Adenovirus-mediated gene transfer of glial cell line-derived neurotrophic factor prevents ischemic brain injury after transient middle cerebral artery occlusion in rats. *J Cereb Blood Flow Metab* 1999; 19: 1336–1344.

- 30 Shimazaki K *et al*. Adeno-associated virus vector-mediated bcl-2 gene transfer into post-ischemic gerbil brain *in vivo*: prospects for gene therapy of ischemia-induced neuronal death. *Gene Therapy* 2000; 7: 1244–1249.
- 31 Beck T *et al*. Brain-derived neurotrophic factor protects against ischemic cell damage in rat hippocampus. *J Cereb Blood Flow Metab* 1994; 14: 689–692.
- 32 Wang JM *et al*. Reduction of ischemic brain injury by topical application of insulin-like growth factor-I after transient middle cerebral artery occlusion in rats. *Brain Res* 2000; 859: 381–385.
- 33 Croll SD, Wiegand SJ. Vascular growth factors in cerebral ischemia. *Mol Neurobiol* 2001; 23: 121–135.
- 34 Abe K *et al*. *In vivo* adenovirus-mediated gene transfer and the expression in ischemic and reperfused rat brain. *Brain Res* 1997; 763: 191–201.
- 35 Inoue M *et al*. Non-transmissible virus-like particle formation by F-deficient Sendai virus is temperature-sensitive and reduced by mutations in M and HN proteins. *J Virol* 2003; 77: 3238–3246.
- 36 Inoue M *et al*. A new Sendai virus vector deficient in the matrix gene does not form virus particles and shows extensive cell-to-cell spreading. *J Virol* 2003; 77: 6419–6429.
- 37 Hayashi K *et al*. Gene therapy for preventing neuronal death using hepatocyte growth factor: *in vivo* gene transfer of HGF to subarachnoid space prevents delayed neuronal death in gerbil hippocampal CA1 neurons. *Gene Therapy* 2001; 8: 1167–1173.